First publ. in: Biochemistry 47 (2008), pp. 13103-13114

ATP Binding Equilibria of the Na^+,K^+-ATPase[†]

Anne Pilotelle-Bunner,[‡,#] Jacqueline M. Matthews,[§] Flemming Cornelius,[||] Hans-Jürgen Apell,[⊥] Pierre Sebban,[#] and Ronald J. Clarke*[,‡]

School of Chemistry, University of Sydney, Sydney NSW 2006, Australia, School of Molecular and Microbial Biosciences, University of Sydney, Sydney NSW 2006, Australia, Department of Physiology and Biophysics, University of Aarhus, DK-8000 Aarhus C, Denmark, Faculty of Biology, University of Konstanz, D-78435 Konstanz, Germany, and Laboratoire de Chimie-Physique, Université Paris-Sud/CNRS, F-91405 Orsay, France

ABSTRACT: Reported values of the dissociation constant, K_d, of ATP with the E1 conformation of the Na^+,K^+-ATPase fall in two distinct ranges depending on how it is measured. Equilibrium binding studies yield values of 0.1−0.6 μM, whereas presteady-state kinetic studies yield values of 3−14 μM. It is unacceptable that K_d varies with the experimental method of its determination. Using simulations of the expected equilibrium behavior for different binding models based on thermodynamic data obtained from isothermal titration calorimetry we show that this apparent discrepancy can be explained in part by the presence in presteady-state kinetic studies of excess Mg^{2+} ions, which compete with the enzyme for the available ATP. Another important contributing factor is an inaccurate assumption in the majority of presteady-state kinetic studies of a rapid relaxation of the ATP binding reaction on the time scale of the subsequent phosphorylation. However, these two factors alone are insufficient to explain the previously observed presteady-state kinetic behavior. In addition one must assume that there are two E1-ATP binding equilibria. Because crystal structures of P-type ATPases indicate only a single bound ATP per α-subunit, the only explanation consistent with both crystal structural and kinetic data is that the enzyme exists as an $(\alpha\beta)_2$ diprotomer, with protein−protein interactions between adjacent α-subunits producing two ATP affinities. We propose that in equilibrium measurements the measured K_d is due to binding of ATP to one α-subunit, whereas in presteady-state kinetic studies, the measured apparent K_d is due to the binding of ATP to both α-subunits within the diprotomer.

Throughout the animal kingdom, the Na^+,K^+-ATPase is responsible for pumping Na^+ and K^+ ions across the plasma membrane and thus maintaining electrochemical potential gradients for both ions across the membrane. A major function of the Na^+ electrochemical potential gradient is to act as a driving force for the uptake of essential metabolites such as glucose and amino acids. Probably the most enduring controversy in the Na^+,K^+-ATPase[1] field is whether the enzyme functions as a monomer, dimer, or higher oligomer (*1, 2*). The idea that the functional unit of the Na^+,K^+-ATPase might consist of an association of two protein monomers was first proposed in the 1970s (*3, 4*). Since then, the idea has had many supporters (*5*−*16*) but also some vocal critics (*17*−*22*) so that the hypothesis of a functional Na^+,K^+-ATPase dimer or higher oligomer has never been universally accepted.

One of the puzzling observations in the Na^+,K^+-ATPase field is that the affinity of the E1 conformation appears to differ depending on whether it is measured by an equilibrium method or a presteady-state kinetic method. From ATP binding studies, a single ATP binding equilibrium with a K_d in the range 0.12−0.63 μM has been detected (*23*−*27*). In contrast, from presteady-state kinetic studies based on enzyme phosphorylation, much higher dissociation constants have been found (K_d in the range 3.5−14 μM) (*28*−*33*).

[†] This work was supported by the Australian Research Council/National Health and Medical Research Council funded Research Network "Fluorescence Applications in Biotechnology and the Life Sciences" (RN0460002). We thank Professor Helge Rasmussen, Royal North Shore Hospital, Sydney, for financial assistance supporting enzyme transport. We also thank the University of Sydney for major infrastructure grants to enable the purchase of the isothermal titration calorimeters. R.J.C. acknowledges with gratitude the Department of Chemistry, Ben-Gurion-University of the Negev, Israel, for a Dozor Visiting Fellowship. J.M.M. is a Viertel Foundation Senior Medical Fellow.

* To whom correspondence should be addressed. Phone: +61 2 9351 4406. Fax: +61 2 9351 3329. E-mail r.clarke@chem.usyd.edu.au.

[‡] School of Chemistry, University of Sydney.

[§] School of Molecular and Microbial Biosciences, University of Sydney.

[||] University of Aarhus.

[⊥] University of Konstanz.

[#] Université Paris-Sud.

[1] Abbreviations: Na^+,K^+-ATPase, sodium and potassium ion-activated adenosine triphosphatase; ATP, adenosine 5′-triphosphate; ADP, adenosine 5′-diphosphate; E1, E2, E1P, and E2P, intermediates of the Na^+,K^+-ATPase pump cycle; EDTA, ethylenediaminetetraacetic acid; CDTA, *trans*-1,2-diaminocyclohexane-*N*,*N*,*N*′,*N*′-tetraacetic acid monohydrate; RH421, *N*-(4-sulfobutyl)-4-(4-(*p*-(dipentylamino)phenyl)butadienyl)-pyridinium inner salt.

Apparent K_d values can also be determined from steady-state kinetic measurements, but these depend on all of the rate constants and equilibrium constants of the enzymatic cycle and, therefore, cannot be compared with the results of equilibrium binding measurements. The question is whether the two different ranges of the K_d value can be explained by the classical monomeric Albers−Post mechanism of Na^+,K^+-ATPase function. One simple explanation for the difference in behavior could be that it is due to Mg^{2+} ions. In equilibrium ATP binding studies, Mg^{2+} must be omitted to avoid phosphorylation, whereas in presteady-state kinetic studies, it must be included to allow phosphorylation. In principle, Mg^{2+} ions could complex ATP in aqueous solution and compete with the enzyme for ATP. A major aim of this article is, therefore, to determine whether or not this is a feasible explanation. To do this requires careful measurements of the equilibrium binding of ATP by both the enzyme and by Mg^{2+} under the same ionic strength and pH conditions. For this, we have used the technique of isothermal titration calorimetry (ITC).

ITC has so far only been applied twice previously to the Na^+,K^+-ATPase; once to measure ouabain interaction with the enzyme (*34*) and once to detect nucleotide binding (*26*). Using this technique, the heat released to or absorbed from the surroundings on ATP binding can be directly measured. In their studies, Grell et al. (*26*) included glycerol in the buffer medium. However, glycerol has not been used in any of the presteady-state kinetic studies, and it could possibly influence the thermodynamics of ATP binding. To allow the analysis described in the previous paragraph, we have carried out here the first ITC measurements of ATP binding to the Na^+,K^+-ATPase in the complete absence of glycerol.

On the basis of these studies, we show that the presence of Mg^{2+} ions would indeed cause a higher apparent K_d of the enzyme for ATP in presteady-state kinetic studies but that this alone is insufficient to explain the large difference in K_d values reported in equilibrium and presteady-state kinetic studies. Another important contributing factor is the inaccurate assumption made either explicitly or implicitly in the majority of presteady-state kinetic studies that the ATP binding reaction is in a rapid equilibrium on the time scale of the subsequent phosphorylation. However, even if such an assumption is not made in the data analysis, we show that presteady-state kinetic data are not consistent with a single ATP binding step. We conclude that in presteady-state kinetic studies two ATP binding steps are occurring, with protein−protein interactions within an $(\alpha\beta)_2$ diprotomer producing two different ATP binding affinities.

MATERIALS AND METHODS

Enzyme. Na^+,K^+-ATPase-containing membrane fragments from shark rectal glands were purified essentially as described by Skou and Esmann (*35*). The specific ATPase activity at 37 °C and pH 7.4 was measured according to Ottolenghi (*36*). The activity of the preparation used was 1679 μmol ATP hydrolyzed h^{-1} (mg of protein)$^{-1}$, and the protein concentration was 4.82 mg/mL. The protein concentrations were determined according to the Peterson modification (*37*) of the Lowry method (*38*) using bovine serum albumin as a standard. For the calculation of the molar protein concentration, a molecular mass for an $\alpha\beta$ unit of the Na^+,K^+-ATPase of 147,000 g mol^{-1} (*39*) was assumed.

Isothermal Titration Calorimetry. Protein samples were dialysed overnight at 4 °C against several liters of the buffer solution to be used for each titration. ATP was dissolved in the same dialysis buffer, and when necessary, the pH was adjusted to match that of the buffer solution by the addition of small volumes of either 1 M NaOH or 1 M HCl. The buffer always contained 130 mM NaCl and 30 mM imidazole, and its pH was always 7.4. For particular experiments, ouabain and EDTA were added, as specified in the Results section. Following dialysis and prior to each titration, the protein samples were degassed and equilibrated at 24 °C. All measurements on the protein were performed at 24 °C using a VP-ITC microcalorimeter (MicroCal Inc., Boston, MA). In all cases, ATP was titrated into the enzyme preparation. The volumes of the injections and the time delay between injections varied according to the experiment. Baseline data were measured by titration of the ATP solution into the appropriate buffer without enzyme, and these were subtracted from the experimental data. Data were analyzed using Origin 7.0 ITC data analysis software (MicroCal Inc.) to determine estimates of the binding constant and the change in enthalpy.

All titrations of ATP, EDTA, and CDTA with $MgCl_2$ were performed at 24 °C using an iTC_{200} microcalorimeter (MicroCal Inc.). In the case of these experiments, $MgCl_2$ was titrated into the ATP, EDTA, or CDTA solutions. Both the solution in the injection syringe and the one in the ITC cell were prepared in the same buffer containing 130 mM NaCl and 30 mM imidazole at pH 7.4 (i.e., exactly the same buffer as that in the enzyme experiments). It was found that for these experiments no degassing of the solutions prior to the titration was necessary. The stirring speed used was 1300 rpm, and the reference power was set at 0.5 μcal/s for the titrations of $MgCl_2$ with CDTA and at 1.0 μcal/s for the titration of $MgCl_2$ with ATP and EDTA. The volume of the ITC_{200} cell was 0.2058 mL. The small constant heat signals remaining after saturation of either ATP, CDTA, or EDTA with Mg^{2+} (due to dilution) were subtracted from the experimental data before calculating binding constants and enthalpy changes.

Simulations. Computer simulations of equilibrium titrations and the concentration dependence of presteady-state kinetic data were performed using the commercially available program Berkeley-Madonna 8.0 (University of California, Berkeley) via a globally convergent variation of the Newton−Raphson method to find the roots of eqs A2, A3, and A8. Computer simulations of the time course of fluorescence changes experimentally observed via stopped-flow were also performed using Berkeley-Madonna 8.0 via the variable step-size Rosenbrock integration method for stiff systems of differential equations. These simulations yield the time course of the concentration of each enzyme intermediate involved as well as the total fluorescence. For the purposes of the simulations, each enzyme intermediate was normalized to a unitary enzyme concentration.

RESULTS

Binding of Mg^{2+} to ATP. If one wishes to compare the ATP binding affinities of the enzyme obtained from equilibrium binding experiments and from presteady-state kinetic studies,

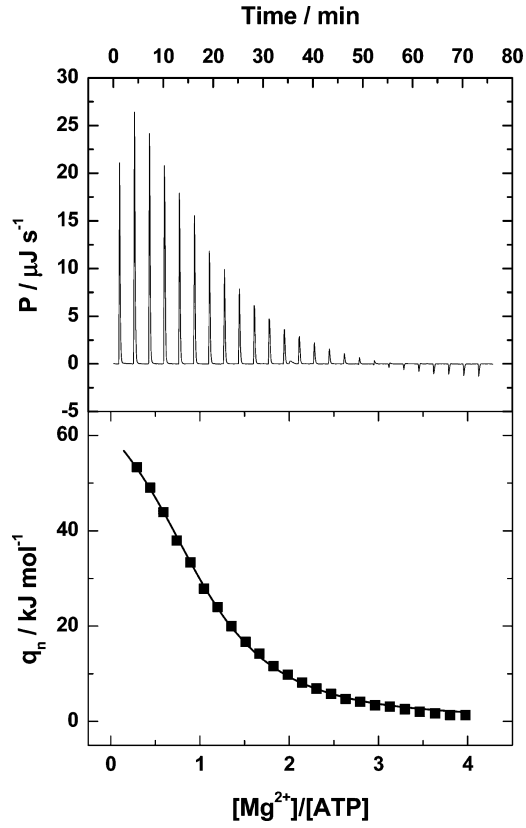

FIGURE 1: Titration of Na_2ATP with $MgCl_2$. The initial concentration of ATP in the ITC cell was 0.25 mM. The buffer of both the ATP and the $MgCl_2$ solutions contained 130 mM NaCl and 30 mM imidazole at pH 7.4. The experiment was conducted at 24 °C. The top panel shows the power, P, in μJ s^{-1} that needs to be applied to the sample cell to maintain isothermal conditions with respect to the reference cell. The bottom panel shows the heat evolved from each $MgCl_2$ injection per mole of Mg^{2+} (obtained from integrating the individual heat pulses of the upper panel) versus the molar ratio of Mg^{2+} to ATP, i.e., $[Mg^{2+}]/[ATP]$. The solid line in the lower panel represents a fit of a 1:1 binding model to the data. The fit yields a Mg^{2+}-ATP binding constant, K_{Mg}, of 1.41 ($\pm$0.06) $\times$ 10^4 M^{-1}. The other thermodynamic parameters derived from the fit are $\Delta H = 75$ ($\pm$2) kJ mol^{-1}, $\Delta G = -23.6$ ($\pm$0.1) kJ mol^{-1}, and $\Delta S = 331$ ($\pm$5) J K^{-1} mol^{-1}.

as we shall do, it is first necessary to establish the dissociation constant for the interaction of ATP with Mg^{2+} ions. The reason for this is that in equilibrium studies Mg^{2+} ions are omitted, but in presteady-state kinetic studies, they are included. Interaction between Mg^{2+} and ATP in the bulk solution could influence the enzyme's apparent affinity for ATP.

The results of a titration of Na_2ATP with $MgCl_2$ are shown in Figure 1. The data can be explained by a simple 1:1 binding equilibrium:

$$Mg^{2+} + ATP \overset{K_{Mg}}{\longleftrightarrow} MgATP$$

The charge on the ATP has been omitted in this equilibrium because ATP is meant to signify all ATP species present in solution at the pH of the experiment, i.e., $HATP^{3-}$, H_2ATP^{2-}, and H_3ATP^{-} as well as ATP^{4-}. The measured binding constant is, thus, an apparent value including the effects of protonation of ATP as well as Na^+ competition under the experimental buffer conditions. Fitting of the data to this binding model yielded the following values: K_{Mg} = 1.41 ($\pm$0.06) $\times$ 10^4 M^{-1} and $\Delta H = 75$ ($\pm$2) kJ mol^{-1}. From these fit parameters one can also calculate that $\Delta G = -23.6$ ($\pm$0.1) kJ mol^{-1} and $\Delta S = 331$ ($\pm$5) J K^{-1} mol^{-1}. Binding of Mg^{2+} by ATP is thus an endothermic reaction under these conditions.

Taking both the pH and NaCl concentration into account as described by O'Sullivan and Smithers (*40*) yields a theoretical apparent value of K_{Mg} of 2.1 $\times$ 10^4 M^{-1} at pH 7.4 and 130 mM NaCl. This value agrees quite well with the experimental value determined here.

Heat Signals Due to ATP Binding to the Na^+,K^+-ATPase. The determination of the dissociation constant for ATP to the Na^+,K^+-ATPase relies on the measurement of the heat of binding of ATP to the enzyme. Any subsequent reactions which might also produce or consume heat and which could, furthermore, perturb the ATP binding equilibrium must be excluded. It is therefore important that enzyme phosphorylation and ATP hydrolysis be prevented. In principle, this can be done by removing all traces of Mg^{2+} and Ca^{2+} from the buffer solution because both ions are capable of acting as ATP cofactors enabling phosphoryl transfer from ATP to the enzyme. In the first instance, therefore, an ATP titration was carried out using a buffer containing 5 mM of the divalent metal ion chelator EDTA. However, the heat signals associated with ATP injection showed a slow return to baseline following the initial exothermic heat pulse, which is not typical of a simple binding reaction. ATP binding alone would be expected to be very rapid, with equilibration occurring on a subsecond time scale (*25, 41, 42*).

In a second ATP titration, we included 1 mM of the specific Na^+,K^+-ATPase inhibitor ouabain in addition to 5 mM EDTA in the buffer solution. Ouabain is known to inhibit the Na^+,K^+-ATPase by binding to a phosphorylated intermediate of the enzyme (E2P) and blocking the enzyme cycle by preventing dephosphorylation (*1, 43, 44*). It, therefore, does not prevent ATP binding or enzyme phosphorylation, but it does prevent enzyme cycling. Under these conditions, it was found that the slow return to baseline was completely eliminated. Much sharper heat pulses were observed. This indicates that the slow return to baseline observed in the previous titration must have been due to Na^+,K^+-ATPase activity and more precisely continuing ATP hydrolysis due to enzyme cycling. Furthermore, if it is true that ATP hydrolysis can only occur in the presence of Mg^{2+} or Ca^{2+} ions, the results of these two titrations indicate that in the first titration 5 mM EDTA must not have been sufficient to completely remove all divalent metal ions from the buffer solution. Some trace amounts must still have been present to allow some enzyme cycling to continue, although at a low rate.

To improve the situation further, we considered replacing EDTA with CDTA. CDTA is also a divalent metal ion chelator, but it has a higher intrinsic binding constant for Mg^{2+} and Ca^{2+} than EDTA (*45, 46*). To test whether this is also the case for the apparent binding constant for Mg^{2+} under our buffer conditions of 130 mM NaCl and pH 7.4, we carried out ITC titrations of both EDTA and CDTA with $MgCl_2$. In fact, we found that EDTA appears to bind Mg^{2+} more strongly than CDTA under our experimental conditions. For EDTA, a $[Mg^{2+}]/[EDTA]$ ratio of approximately 3 is sufficient to completely saturate all of the EDTA with Mg^{2+} ions. In the case of CDTA, one must continue the titration

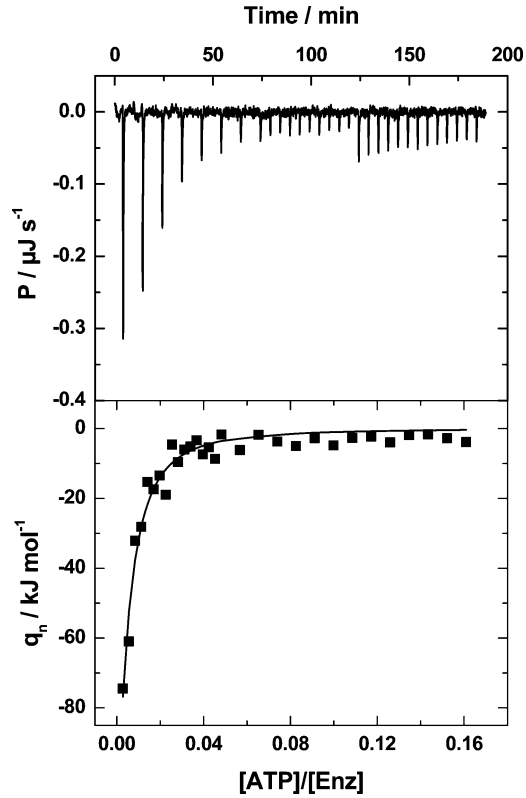

FIGURE 2: Titration of shark Na^+,K^+-ATPase-containing membrane fragments from shark rectal gland with ATP. The initial concentration of Na^+,K^+-ATPase in the ITC cell was 13.7 μM. The buffer of both the Na^+,K^+-ATPase suspension and the ATP solution contained 130 mM NaCl, 5 mM EDTA, 1 mM ouabain, and 30 mM imidazole at pH 7.4. The experiment was conducted at 24 °C. The upper and lower panels have the same meaning as for Figure 1 except that q_n here is the heat evolved per mole of ATP injected. The negative value of P indicates heat evolution, i.e., an exothermic reaction. The increase in the power of the heat pulses at 125 min is due to an increase in the injection volume at this point in order to saturate the available ATP sites. The solid line in the lower panel represents a fit of a binding model with one class of sites to the data. This model is similar to the monomer model described in the appendix, except that the possibility of a variable number of ATP binding sites per enzyme molecule was included to take into account the possibility of inaccessible sites. The fit yields an ATP dissociation constant, K_d, of 0.27 ($\pm$0.09) μM.

to a $[Mg^{2+}]$/[CDTA] ratio of greater than 8 to achieve the same level of saturation.

A further experimental finding from the titration of enzyme with ATP in the presence of EDTA (but in the absence of ouabain) was that the slow return to baseline became more pronounced as the titration proceeded and the ATP concentration increased. This can easily be explained by competition between EDTA and ATP for the trace amounts of Mg^{2+} available. By including 1 mM ouabain in the buffer medium, however, any small amount of phosphorylated enzyme that is produced is blocked in the phosphorylated state and does not continue cycling.

Binding of ATP to the Na^+,K^+-ATPase. The results of a titration of shark Na^+,K^+-ATPase with ATP in a pH 7.4 30 mM imidazole buffer containing 5 mM EDTA and 1 mM ouabain are shown in Figure 2. A simple binding model with one class of sites was fitted to the data, leading to an apparent ATP dissociation constant of 0.27 ($\pm$0.09) μM. This value agrees well with previously reported values using other techniques, i.e., 0.12$-$0.24 μM (*23*$-$*25*). Unfortunately, a reliable value of the enthalpy of binding could not be determined because of insufficient data points at low ATP/enzyme molar ratios. However, from the initial data point of the titration, one would expect ΔH to be of the order of $-$ 75 kJ mol^{-1}.

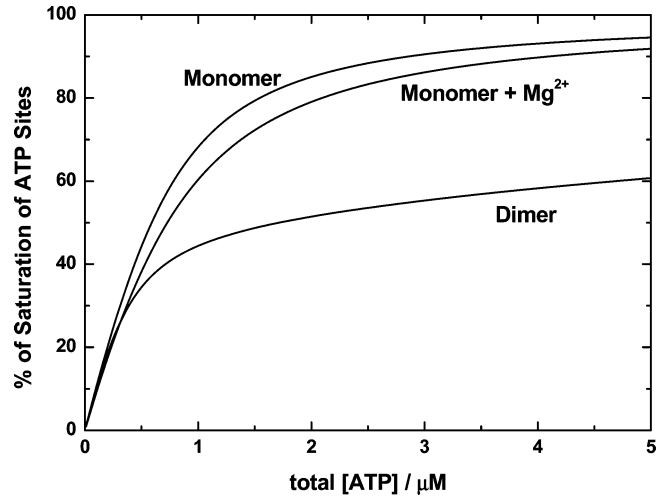

FIGURE 3: Simulated dependence of the percentages of saturation of the ATP sites of the Na^+,K^+-ATPase for a monomer model with and without the presence of Mg^{2+} ions and a cooperative dimer model. The percentage saturations are given by S (see Appendix) multiplied by 100. The values of all of the parameters used were $K_1 = 4 \times 10^6$ M^{-1}, $K_2 = 1.43 \times 10^5$ M^{-1}, $K_{Mg} = 1.41 \times 10^4$ M^{-1}, and $K_{MA} = 2.56 \times 10^6$ M^{-1}. The total protein concentration (i.e., the concentration of $\alpha\beta$ protomers) used was 0.68 μM, which was chosen to agree with the conditions of the equilibrium titrations published in ref *41*. For the monomer simulation with Mg^{2+} ions, a Mg^{2+} concentration of 5 mM was used.

Model Simulations of the Degree of Saturation of the ATP Sites. To test whether competition between free Mg^{2+} and enzyme for ATP could account for the different K_d values reported in the literature from equilibrium and presteady-state measurements, we have carried out simulations of the expected variation of the total saturation of the ATP sites, S, for a monomeric model in the presence and absence of Mg^{2+} ions. The results of the simulations are shown in Figure 3. The equations used for the simulations are described in the Appendix.

The results of these simulations (see Figure 3) show that a monomeric model in the absence of Mg^{2+} ions predicts a hyperbolic saturation curve of the ATP sites, with half-saturation occurring in the submicromolar range, in agreement with experimental observations (*23*$-$*25, 27*). One needs to be aware here that the actual half-saturating concentration depends on how the theoretical or experimental data are plotted. Strictly speaking, one should plot the percentage saturation of the ATP sites versus the free ATP concentration. If this is done, the half-saturating free ATP concentration exactly equals the K_d for ATP binding (in the case of the simulations, 0.25 μM was the value used). More commonly, however, the percentage saturation is plotted against the total concentration of ATP because this is a more directly accessible quantity. Therefore, this is the way the simulations in Figure 3 have been plotted. The half-saturating total ATP concentration, however, does not equal K_d. In our monomer simulation, the half-saturating total ATP concentration occurs at 0.59 μM, more than twice the actual K_d. Therefore, one needs to be wary of this fact when reporting K_d values or interpreting literature data.

A significant difference between the conditions of equilibrium binding studies and presteady-state kinetic studies is that Mg^{2+} ions are excluded in equilibrium studies but included in presteady-state kinetic studies. Therefore, the possibility must be considered that the presence of Mg^{2+} ions could be modifying the enzyme's apparent ATP binding affinity and that this could account for the higher value of K_d generally observed in presteady-state kinetic studies. Certainly, Mg^{2+} ions in the bathing solution could bind ATP and compete with the enzyme. This would be expected to increase the enzyme's apparent K_d for ATP. However, one must also consider that the enzyme could bind the MgATP complex. Simulations taking into account both of these effects have also been carried out, and the results are shown in Figure 3. The equations used are described in the Appendix.

There is some disagreement in the literature concerning the relative dissociation constants of free nucleotide and Mg-nucleotide complex for the enzyme. Campos and Beaugé (*47*) report K_d values of 1.52 μM and 0.36 μM for free ATP and MgATP, respectively, i.e., they consider that the complex binds to the enzyme approximately a factor of 4 more strongly than free ATP. According to the data of Fedosova et al. (*41*), however, the Mg^{2+} complex of ADP should bind to the enzyme a factor of 1.6 more weakly than free ADP. Grell et al. (*26*) found that the affinity of ADP for the enzyme is reduced by a factor of 4 in the presence of 3 mM $MgCl_2$. Since there is no possible way that a Mg^{2+}-induced increase in ATP affinity could explain the lower affinity observed for ATP in presteady-state kinetic studies where Mg^{2+} is present, for the purposes of our simulations we have only considered the case that the MgATP complex binds to the enzyme more weakly than free ATP. We have chosen a value of K_1 of 4×10^6 M^{-1}, on the basis of previous measurements (*16, 25, 41, 42*) for the binding of free ATP. For the binding of the MgATP complex, we have used a value of K_{MA} of 2.56×10^6 M^{-1}. This value is based on the 1.56-fold lower K_d found by Fedosova et al. (*41*) for the MgADP complex relative to free ADP.

The results of these calculations indicate that the presence of 5 mM Mg^{2+} would indeed be expected to increase the enzyme's apparent K_d for ATP. On the basis of the simulations shown in Figure 3, one would expect a half-saturating total ATP concentration of 0.73 μM, in comparison to 0.59 mM in the absence of Mg^{2+}. For these simulations, the enzyme concentration used was 0.68 μM. This value was chosen to reproduce the conditions of the radioactivity-based equilibrium binding assay of Fedosova et al. (*41*). If the enzyme concentration is reduced by a factor of 10 to reproduce the conditions of the fluorescence-based stopped-flow kinetic measurements of Kane et al. (*32*), corresponding simulations show that for the monomeric enzyme in the presence of 5 mM $MgCl_2$ the expected half-saturating total ATP concentration would be 0.42 μM. This value is still more than an order of magnitude lower than the average value of the apparent K_d determined from presteady-state kinetic studies, i.e., approximately 8 μM. Therefore, a direct competition between Mg^{2+} and enzyme for ATP cannot alone explain the different ATP binding affinities observed in presteady-state kinetic and equilibrium studies.

DISCUSSION

The isothermal titration calorimetric data we have presented here indicate that ATP can bind exothermically to the E1 conformation of the Na^+,K^+-ATPase with a dissociation constant of 0.27 ($\pm$0.09) μM. This value is consistent with previous studies using other methods (*23−25, 27*). Under the same pH and ionic strength conditions, Mg^{2+} was found to bind to ATP in free solution with a dissociation constant of 71 ($\pm$3) μM. Together, the data obtained has enabled us to analyze the question of the effect that Mg^{2+} would be expected to have on ATP binding in presteady-state kinetic measurements if the enzyme existed prior to mixing with ATP in a monomeric form, i.e., $\alpha\beta$ protomer.

Simulations of the degree of saturation of the ATP sites for a monomeric enzyme model (see Figure 3) showed that direct competition between Mg^{2+} and the enzyme cannot alone explain the differences observed between equilibrium and presteady-state kinetic results. Another possibility to explain the difference is that the mechanism used to describe the sequence of ATP binding when analyzing the equilibrium and presteady-state kinetic data is incorrect. A possible mechanism, which could in principle explain a lower K_d from equilibrium versus presteady-state kinetic measurements, is shown below:

$$E1 + ATP \leftrightarrow E1 \cdot ATP \leftrightarrow E1' \cdot ATP \rightarrow E2P$$

A mechanism similar to this has been proposed by Jencks and co-workers (*48, 49*) based on quenched-flow measurements performed on sheep kidney Na^+,K^+-ATPase. The most important difference between this mechanism and the classical Albers−Post mechanism is that it includes a rate-limiting conformational change of the enzyme−ATP complex, E1·ATP $\leftrightarrow$ E′·ATP, prior to a rapid phosphoryl transfer reaction to produce the phosphoenzyme. Because the reaction E1·ATP $\leftrightarrow$ E1′·ATP is assumed to be the rate-determining step, the maximum observed rate constant of phosphorylation when starting in the E1 state must be given by the rate constant of this reaction. Furthermore, the concentration of free ATP required to achieve the half-saturating observed rate constant (i.e., K_d) must be given by the ATP concentration required to achieve half-saturation of the species immediately before the rate-determining step, i.e., E1·ATP. In contrast, in equilibrium ATP titrations one would measure the total degree of saturation of the enzyme with ATP, i.e., the sum of the degrees of saturation of E1·ATP and E1′·ATP. As long as the equilibrium constant of the reaction E1·ATP $\leftrightarrow$ E1′·ATP is greater than 1, on the basis of such a mechanism the apparent K_d determined by equilibrium titrations would be lower than that determined by presteady-state kinetic measurements, i.e., in qualitative agreement with experimental observations.

However, if this mechanism were correct, then the maximum observed rate constant achievable for phosphorylation of the enzyme should depend on whether or not the enzyme is preincubated with ATP. If the E1·ATP $\leftrightarrow$ E1′·ATP reaction is rate-determining when starting in the E1 state, then pre-equilibration with ATP such that the enzyme starts in E1′·ATP should lead to a significantly higher observed rate constant of phosphorylation. However, stopped-flow kinetic investigations of the formation of E2P using enzyme from both pig and rabbit kidney

labeled with the fluorescent probe RH421 have shown that the maximum observed rate constant is always in the range 180−200 s^{-1}, whether the enzyme is preincubated with Na^+, ATP, or Na^+ and ATP together (*50*). Comparison of RH421 stopped-flow kinetic measurements with quenched-flow measurements of the formation of E1P at the same temperature (24 °C) showed complete agreement (*32*), indicating that the E1P → E2P transition is very fast under these conditions and does not contribute significantly to the observed rate constants measured via stopped-flow with the probe RH421.

A further possibility worth considering would be that a conformational change of the enzyme−ATP complex exists prior to phosphorylation, but that the conformational change requires the presence of all relevant substrates and cofactors, i.e., Na^+, Mg^{2+}, and ATP. If this were the case, then kinetic measurements in which the enzyme was preincubated with only two or less of the substrates or cofactors could never reveal the existence of such a conformational change. However, in such a situation the conformational change would not occur in equilibrium measurements in which Mg^{2+} ions are excluded. Therefore, if the conformational change was rate-limiting, equilibrium and kinetic measurements should yield the same K_d value for ATP. Alternatively, if the conformational change was not rate-limiting for phosphorylation, then, regardless of the equilibrium constant of the conformational change, it would always shift the initial ATP binding equilibrium to the right, i.e., in the direction of the enzyme−ATP complex. This should then lead to the observation of a lower K_d in presteady-state kinetic experiments relative to equilibrium experiments. This is the exact opposite of the experimentally observed behavior. Therefore, a conformational change requiring all substrates and cofactors prior to phosphorylation can be excluded as explanation of the results.

A further argument against any mechanism involving a conformational change (rate-determining or not) of the enzyme−ATP complex is that they all predict only a single ATP binding step. However, the careful analysis of the observed rate constants and the amplitudes of presteady-state kinetic data by a number of researchers have shown in fact that evidence for two ATP binding steps can be detected (*12, 16, 51*). This will be discussed further later. For these reasons, a conformational change of an enzyme−ATP complex must be rejected as an explanation of the difference in ATP binding behavior observed in equilibrium and presteady-state kinetic measurements.

Another possibility for explaining the difference in the K_d values determined by equilibrium and presteady-state kinetic methods is an inaccurate assumption in the data analysis. In many presteady-state kinetic studies (*28−33*), the K_d value has been determined by the fitting of an equation of the following form to the experimentally determined observed rate constants, k_{obs}, (or reciprocal relaxation times) for enzyme phosphorylation or formation of the E2P state:

$$k_{obs} = k_p \cdot \frac{[\mathrm{ATP}]}{K_d + [\mathrm{ATP}]} \qquad (1)$$

where k_p is the rate constant for phosphorylation. The derivation of this equation requires the assumption that ATP binding can continually adjust to a new equilibrium as it is perturbed by the phosphorylation reaction. If this assumption is not justified, this could perhaps explain the apparent discrepancy between equilibrium and presteady-state kinetic measurements. To test the validity of this assumption, one needs to calculate the expected reciprocal relaxation time, $1/\tau$, for the establishment of the ATP binding equilibrium. Under conditions of excess ATP over enzyme, this is given by the following equation (*52*):

$$1/\tau = k_+[\mathrm{ATP}] + k_- \qquad (2)$$

where k_+ is the rate constant for ATP binding to the enzyme, and k_- is the rate constant for ATP dissociation. The value of k_- in the absence of Mg^{2+} has been directly measured by rapid filtration studies to be 13 s^{-1} (*41*). The estimation of a value for k_+ is more difficult. However, on the basis of the value of k_- and assuming a K_d value of 0.42 μM (the theoretical value determined here in the presence of Mg^{2+} based on the equilibrium ITC results), one can estimate a value for k_+ of 3.1 × 10^7 M^{-1} s^{-1}. According to eq 2, on the basis of these values of k_+ and k_- the expected values of $1/\tau$ at different ATP concentrations would be 3,108 s^{-1} (100 μM), 323 s^{-1} (10 μM), 44 s^{-1} (1 μM), and 16 s^{-1} (0.1 μM). If one compares these values with the value of the phosphorylation rate constant, k_p, which has been determined to be in the range 180−200 s^{-1} (*16, 30−33*) when the enzyme is fully saturated by ATP, one would expect the assumption of a rapid adjustment of the ATP binding equilibrium to become increasingly bad as the ATP concentration decreases, with the assumption starting to break down at an ATP concentration of less than 10 μM.

To test the effect of this inaccurate assumption on the analysis of presteady-state kinetic data, we have simulated the time course of presteady-state kinetic transients based on a single ATP binding step with an apparent K_d of 0.42 μM (taking into account the presence of Mg^{2+}) and fitted the theoretical transients to a single exponential time function to derive the expected values of k_{obs}. All of the equations necessary for carrying out simulations based on a one-site monomer model of the Na^+,K^+-ATPase have been described elsewhere (*16*). The expected dependence of k_{obs} on the total ATP concentration derived from these simulations is shown in Figure 4. The half-saturating total concentration of ATP (i.e., which is generally reported as the apparent K_d) is found to be in the range 3−4 μM. It is clear that this value is significantly larger than the apparent value of K_d in the presence of 5 mM Mg^{2+} of 0.42 μM used to generate the theoretical data, and the difference is even larger when one compares with the K_d value directly measured from equilibrium titrations of 0.27 μM. Therefore, this type of data analysis, which is the one most commonly used for presteady-state investigations of Na^+,K^+-ATPase phosphorylation, results in a severe overestimation of the value of K_d. The inappropriate assumption of rapid ATP binding pre-equilibrium is, therefore, an important factor which would also contribute to the much higher values of K_d reported from presteady-state kinetic studies in comparison to equilibrium binding studies. Nevertheless, the apparent K_d values reported from presteady-state studies are often even larger than the 3−4 μM range predicted here from theoretical calculations based on equilibrium binding data. Values reported in the literature cover the range 3.5−14 μM (*28−33*). This suggests that there may be a further reason for the high K_d values found in presteady-state kinetic studies.

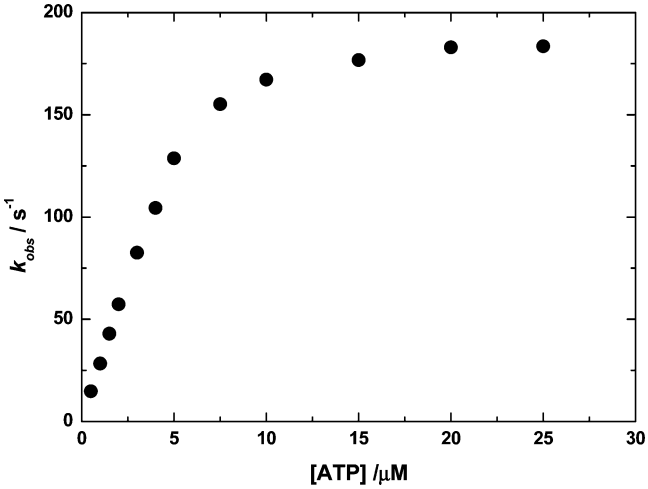

FIGURE 4: Simulated dependence of the observed rate constant, k_{obs}, (or reciprocal relaxation time) of RH421 stopped-flow fluorescence transients on the total concentration of ATP after mixing. The simulations were based on a single-site monomer model. The values of the rate constants used were 13 s^{-1} (E1ATP → E1 + ATP; (*41*)), 31 μM^{-1} s^{-1} (E1 + ATP → E1ATP), 173 s^{-1} (E1ATP → E2P; (*16*)), 5 s^{-1} (E2P → E1ATP, i.e., dephosphorylation followed by rebinding of ATP; (*16*)) and 75 s^{-1} (E2PATP → E1ATP; (*16*)). The ATP binding rate constant was chosen to be consistent with the K_d value calculated here based on equilibrium titrations of 0.42 μM. The dissociation constant of ATP to the E2P state was taken as 143 μM (*16*). The fluorescence level of the E1 and E1ATP states were defined as 1.0. On the basis of the experimentally observed increase in fluorescence, the fluorescence level of the E2P state was defined as 2.14 (*16*). All of the equations used in carrying out the simulations are described in the Appendix of ref *16*.

In fact, the analysis of presteady-state kinetic data does not necessarily require the assumption of a rapid ATP binding equilibrium. An alternative approach, avoiding this assumption, is to numerically simulate the experimental curves using the complete set of differential rate equations (i.e., including differential rate equations for ATP binding and release) appropriate to the kinetic model being tested. This approach was recently used by us (*16*) to show that a single site binding model with a K_d of 7.0 μM could not explain the ATP concentration dependence of the amplitudes of the experimentally observed stopped-flow traces, even though it could reproduce relatively well the time course of the observed fluorescence change and its acceleration with increasing ATP concentration. The question here is whether a single site model can explain the amplitudes and the kinetics of the stopped-flow results if one assumes a K_d value consistent with that obtained from equilibrium measurements, i.e., 0.42 μM (taking into account the effect of Mg^{2+} competition). All of the equations necessary for carrying out simulations based on a one-site monomer model of the Na^+,K^+-ATPase have been described elsewhere (*16*). A comparison between simulations based on this model and experimentally observed stopped-flow traces (reproduced from ref *16*) is shown in Figure 5. This comparison indicates that there are huge differences between the experimental traces and those predicted by a one-site monomer model based on the equilibrium data, particularly at low ATP concentrations, i.e., 1 μM and below. Good agreement is only obtained at very high ATP concentrations, e.g., 500 μM, when the enzyme would be saturated by ATP for any value of K_d of 10 μM and below. This comparison indicates that even if no assumption of an ATP equilibrium is used in the data analysis, a large discrepancy still exists between observed presteady-state kinetic data and the behavior that would be predicted by a single site model based on the K_d for ATP of 0.42 μM expected based on the equilibrium data.

If the presteady-state kinetic data cannot be explained within the framework of a single ATP binding equilibrium, then one is forced to conclude that there are actually two separate ATP binding equilibria. Crystal structural data on the related P-type ATPase, the sarcoplasmic reticulum Ca^{2+}-ATPase, only provide evidence for a single ATP binding site per enzyme molecule (*53*). The only consistent explanation for two ATP binding equilibria but still with a 1:1 stoichiometry between ATP and the enzyme is a cooperative binding of ATP to the two α-subunits of an $(\alpha\beta)_2$ diprotomer, as described by Figure 6.

In Figure 7, the result of a simulation of the degree of saturation of an enzyme dimer, S_{dim}, (i.e., the fraction of enzyme in the E1ATP:E1ATP state) as a function of the total ATP concentration is shown. The model used for this simulation is shown diagrammatically in Figure 6. The equations used for the simulation are described in the Appendix. The graph shows that S_{dim} rises much more slowly with increasing ATP concentration than the total saturation of the ATP sites, S, for the same dimer model (cf. the Dimer curve in Figure 3). The simulations in Figures 3 and 7 are shown over the same ATP concentration range for ease of comparison. However, if one extends the simulations over a larger concentration range it is found that 50% of the enzyme is present as E1ATP:E1ATP at a total ATP concentration of 15 μM, whereas 50% of the ATP sites are occupied already at 1.7 μM. These numbers are based on a protein concentration of 0.68 μM, as used by Fedosova et al. (*41*). If the enzyme concentration is reduced by a factor of 10 to reproduce the conditions of the presteady-state kinetic experiments of Kane et al. (*32*), the corresponding half-saturating total ATP concentrations are 14 μM for E1ATP:E1ATP and 1.4 μM for the ATP sites. The difference in the concentration range over which dimers are saturated by ATP as opposed to the concentration over which the ATP sites within a dimer are saturated can easily be explained if one considers the hypothetical case where half of all of the sites are occupied. Because in the dimer model the first ATP that binds to a dimer is assumed to bind with high affinity and the second with low affinity, dimers with only one ATP binding site occupied would form preferentially to dimers with both sites occupied. If one imagines a situation where every dimer has one ATP molecule bound, the total saturation of the sites would be 50%, but the percentage of completely saturated dimer would still be 0%. Thus, S_{dim} must rise more slowly than S for the dimer model.

The observed rate constant (or reciprocal relaxation time) found in presteady-state kinetic studies of enzyme phosphorylation (*28*−*33*) shows an ATP concentration dependence, which agrees approximately with the ATP concentration dependence of S_{dim} shown here (see Figure 7). These studies have yielded higher apparent ATP dissociation constants than equilibrium binding studies, i.e., 3.5−14 μM from presteady-state kinetic studies in comparison to 0.12−0.63 μM from binding studies. The higher ATP concentration required for saturation in presteady-state kinetic studies suggests, therefore, that the formation of a fully saturated enzyme dimer, E1ATP:E1ATP, is required for the

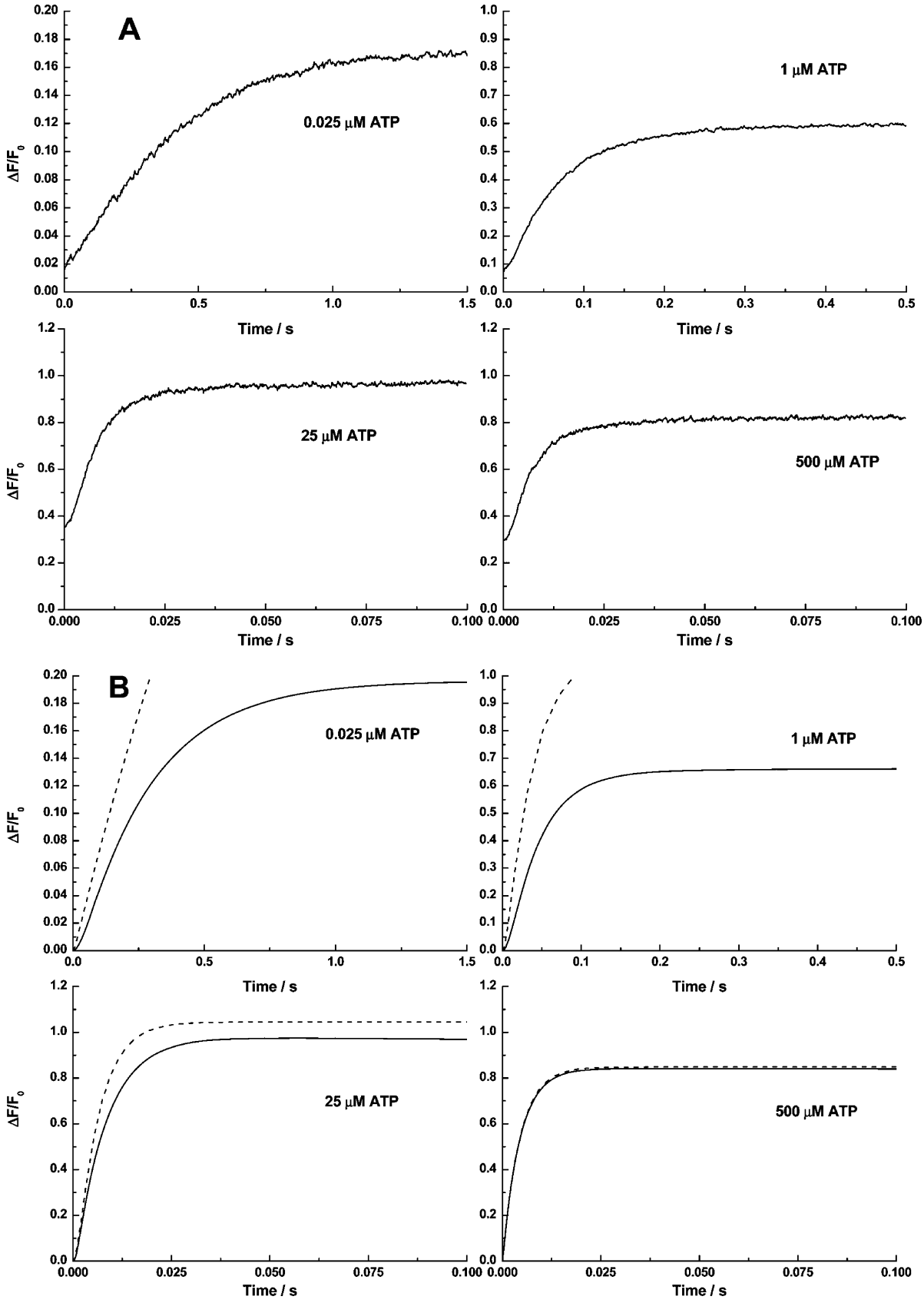

FIGURE 5: (A) Stopped-flow fluorescence transients (reproduced from ref *16*) of Na^+,K^+-ATPase from pig kidney noncovalently labeled with RH421 (75 nM, after mixing). Na^+,K^+-ATPase (10 μg/mL or 68 nM, after mixing) was rapidly mixed with an equal volume of a solution containing varying concentrations of Na_2ATP. Both the enzyme suspension and the Na_2ATP solutions were prepared in a buffer containing 130 mM NaCl, 30 mM imidazole, 5 mM $MgCl_2$, and 1 mM EDTA (pH 7.4, 24 °C). All further experimental procedures can be found in ref *16*. (B) Kinetic simulations of the experimental fluorescence transients based on a single-site monomer model (dashed line) and a dimer model (solid line, reproduced from ref *16*). The values of the rate constants used for the simulations based on the monomer model are given in the caption to Figure 4. All of the equations used in carrying out the simulations are described in the Appendix of ref *16*.

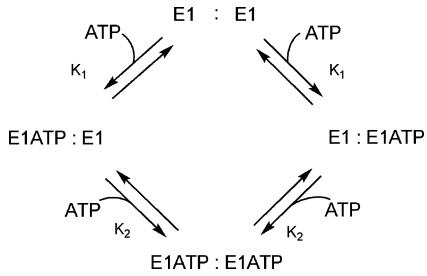

FIGURE 6: Cooperative dimer model of ATP binding. K_1 and K_2 represent the binding constants of the first and second ATP binding steps. The species E1ATP:E1 and E1:E1ATP are chemically equivalent, but they are included for statistical reasons (i.e., because E1:E1 has two available ATP binding sites). For anticooperative ATP binding, $K_1 > K_2$.

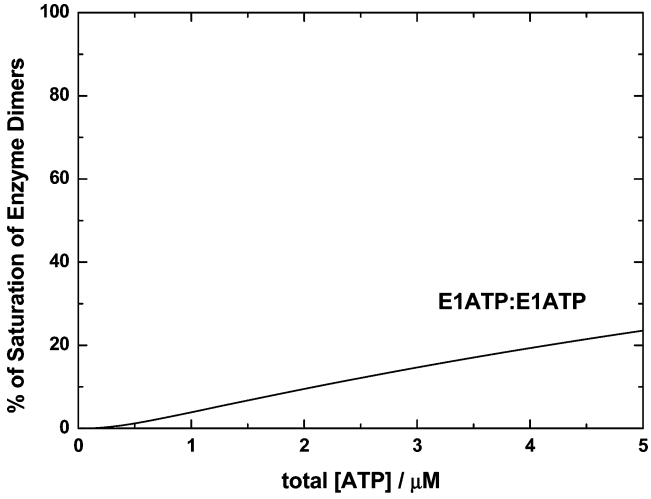

FIGURE 7: Simulated dependence of the percentage of enzyme in the E1ATP:E1ATP state for a cooperative dimer model. The percentage saturations are given by S_{dim} (see Appendix) multiplied by 100. The values of all of the parameters used were $K_1 = 4 \times 10^6\ M^{-1}$ and $K_2 = 1.43 \times 10^5\ M^{-1}$. The total protein concentration (i.e., the concentration of $\alpha\beta$ protomers) used was 0.68 μM, which was chosen to agree with the conditions of the equilibrium titrations published in ref *41*.

maximum rate of phosphorylation, as previously suggested (*16*). In Figure 5B (solid curve), simulated stopped-flow fluorescence transients reflecting the kinetics of the reaction $E1(Na^+)_3 + ATP \rightarrow E2P$ based on the dimer model are shown. These have been reproduced from ref *16*. Comparison of these simulated curves with the experimentally obtained transients (Figure 5A) and with the simulations carried out here based on the equilibrium data and a one-site monomer model (dashed curve in Figure 5B) shows that, in contrast to the monomer model, the dimer model reproduces the experimental behavior very well.

One point worthy of further consideration, however, is the effect that ATP has on the dephosphorylation reaction. In the simulations for both the monomer and dimer models presented here and in our earlier work (*16*), an ATP-induced acceleration of the dephosphorylation reaction by binding to E2P was assumed in order account for the drop in fluorescence amplitude of the observed RH421 stopped-flow transients at high ATP concentrations (hundreds of micromolar range). However, this could alternatively be explained by an ATP-induced decrease in the sensitivity of RH421 to the release of Na^+ from E2P. To decide which of these two explanations is correct requires further experimentation.

On the basis of the analysis presented here, it seems most likely that the different ATP concentration required for half-saturation in equilibrium and presteady-state kinetic studies is due not only to different Mg^{2+} concentrations but also to a different concentration dependence of the experimental observable, i.e., concentration of bound ATP or observed rate constant, respectively. In binding studies, one is measuring the degree of total occupation of the enzyme's ATP binding sites, whereas in presteady-state kinetic studies, the observed rate constant depends on the degree of occupation of an enzyme dimer. Both of these have different ATP concentration dependences (cf. Figures 3 and 7).

Recent crystal structure data (*54*) has shown that the structure of the Na^+,K^+-ATPase is very similar to that of its related enzyme, the Ca^{2+}-ATPase of sarcoplasmic reticulum. This provides strong support for the validity of comparisons between the two enzymes. Therefore, it is important at this stage to mention the work of Møller et al. (*55*) on the sarcoplasmic reticulum Ca^{2+}-ATPase. This enzyme occurs in the sarcoplasmic reticulum membrane with a high density and forms an aggregated state, similar to the Na^+,K^+-ATPase in the plasma membrane. Møller et al. (*55*) investigated the effect of protein−protein interactions on the enzyme's kinetics by comparing the kinetic behavior of aggregated vesicular Ca^{2+}-ATPase and monomeric enzyme solubilized using the detergent $C_{12}E_8$. What they found was that detergent solubilization decreased the enzyme's ATP affinity. For the aggregated enzyme, they measured an ATP K_d of 2 μM, whereas for the monomeric enzyme, they determined a K_d of 7 μM. This result suggests that, for the Ca^{2+}-ATPase, protein−protein interactions in the native membrane enhance the enzyme's affinity for ATP. The same could be true of the Na^+,K^+-ATPase. This would imply that the low K_d of around 0.2 μM obtained from equilibrium titrations in the absence of Mg^{2+} actually corresponds to ATP binding to an $(\alpha\beta)_2$ protein dimer, whereas the high K_d of around 10 μM obtained from presteady-state kinetic studies is due to ATP binding to disaggregated protein monomers, i.e., individual $\alpha\beta$ protomers. The conformational change of the enzyme, which brings about the change in the enzyme's ATP affinity could then be attributed to protein disaggregation within the membrane. If this is true, then the species E1ATP:E1ATP, so far described here as a dimeric species, would actually represent a disaggregated dimer, i.e., in fact simply two neighboring protein monomers, both of which have ATP bound but with no interaction between them.

There are both kinetic and structural data that would support such a conclusion. First of all, in the two gear pumping model, which we recently demonstrated could explain stopped-flow kinetic data over an ATP concentration range of approximately 5 orders of magnitude (*16*), the higher gear of pumping following the binding of ATP to both $\alpha\beta$ protomers of the $(\alpha\beta)_2$ diprotomer involved a synchronous pumping by each $\alpha\beta$ protomer. The simplest way that each $\alpha\beta$ protomer could pump with the same rate constant would be if they were completely independent of one another, i.e., disaggregated with no interactions between them. Protein disaggregation following ATP binding is also supported by X-ray crystal structural data obtained on the Ca^{2+}-ATPase. Olesen et al. (*53*) have shown that an important role of ATP in the function of P-type ATPases, apart from phosphorylating the enzyme, is to maintain the cytoplasmic domains

in a compact closed conformation. In the absence of ATP, the cytoplasmic domains of the E1 conformation are much more widely spread, and because of the high density of these enzymes in specialized membranes such as in the kidney and the shark rectal gland used here, this could easily lead to protein−protein interactions within the membrane and consequent changes in nucleotide binding affinity. Whether the dimeric species that we propose occur at low ATP concentrations are due to specific protein−protein interactions or whether they are simply due to the close proximity of pump molecules to each other because of their high density in some tissues remains unclear. If the interaction were nonspecific, the more fashionable term of macromolecular crowding may be a more appropriate description of the interaction rather than using the term dimer. Therefore, although we have used the term dimer throughout this article, we do not necessarily mean to imply a specific interaction between defined pairs of protein molecules. Nevertheless, a recent paper by Mimura et al. (*56*), in which they report the isolation of stable $(\alpha\beta)$, $(\alpha\beta)_2$, and $(\alpha\beta)_4$ forms of the enzyme from dog kidney, would seem to lend support to the argument that the interaction may be specific.

Finally, it must be pointed out that in other models of the Na^+,K^+-ATPase mechanism incorporating a dimer or higher oligomer as the functional unit Taniguchi, Froehlich, and their co-workers (*11, 14, 57*) have considered that individual protein monomers within the oligomeric unit undergo asynchronous reaction such that each oligomer contains a combination of different enzyme states. This would appear to be inconsistent with the existence of the species E1ATP:E1ATP. However, as stated earlier, we consider that this is not a true dimeric species, but rather two neighboring protein monomers with ATP bound to both. In contrast, the species E1:E1, E1:E1ATP, and E1ATP:E1 are considered here to be true dimeric species with interactions between the two monomers. Thus, when a true dimeric state exists, such as E1:E1ATP, the individual protein monomers are indeed asynchronous, as Taniguchi and Froehlich have suggested. The major novelty in the enzyme mechanism that we are proposing is that we consider the enzyme to be neither strictly monomeric nor strictly oligomeric, but rather that it can undergo a transition from an oligomeric to a monomeric form and that this transition is mediated by an interaction with ATP.

APPENDIX

Single Site Model without Mg^{2+}. Binding of ATP to the $E1(Na^+)_3$ conformation of the enzyme can be described by the equilibrium

$$E1 + ATP \overset{K_1}{\longleftrightarrow} E1ATP$$

where K_1 is the apparent binding constant of ATP to the enzyme. Taking into account mass balance of the enzyme, the concentration of E1ATP is

$$[E1ATP] = \frac{K_1[E]_{tot}[ATP]}{1 + K_1[ATP]} \qquad (A1)$$

where $[E]_{tot}$ is the total concentration of enzyme. Taking into account mass balance for ATP, the free ATP concentration, [ATP], is related to the total enzyme concentration and the total ATP concentration, $[ATP]_{tot}$ by

$$[ATP] + \frac{K_1[E]_{tot}[ATP]}{1 + K_1[ATP]} - [ATP]_{tot} = 0 \qquad (A2)$$

Solving for the roots of eq A2 allows [ATP] to be calculated and then, by substitution into eq A1, [E1ATP] as well.

For the analysis of equilibrium titrations and presteady-state kinetic data, the degree of saturation, S, of the ATP binding sites as a function of [ATP] needs to be calculated. S is given by $[E1ATP]/[E]_{tot}$. [E1ATP] can be determined from eq A1 after solving for [ATP] from eq A2.

Single Site Model Including Mg^{2+}. Equilibrium binding assays can never yield the apparent K_d of the enzyme for ATP in the presence of Mg^{2+} because under these conditions, the enzyme would immediately undergo phosphorylation and continue cycling until all the ATP was consumed. Therefore, the equilibrium condition can never be fulfilled. However, if sufficient equilibrium binding information is available for the individual equilibria involved from separate binding studies, a theoretical K_d can be calculated for comparison with that obtained in presteady-state kinetic studies.

Under these conditions it is necessary to consider three separate equilibria:

$$E1 + ATP \overset{K_1}{\longleftrightarrow} E1ATP$$

$$Mg^{2+} + ATP \overset{K_{Mg}}{\longleftrightarrow} MgATP$$

$$E1 + MgATP \overset{K_{MA}}{\longleftrightarrow} E1MgATP$$

In theory, there is a fourth equilibrium, i.e., the binding of Mg^{2+} ions to the enzyme. However, experimentally the Mg^{2+} concentration of the bulk solution is far in excess of the enzyme so that the small amount of Mg^{2+} lost from the bulk by binding to the enzyme is negligible. We also assume that Mg^{2+} is far in excess of the ATP concentration so that the free Mg^{2+} concentration can be approximated by the total concentration, $[Mg^{2+}]_{tot}$. Taking into account mass balance for ATP under these conditions, [ATP] is related to $[E]_{tot}$, $[Mg^{2+}]_{tot}$, and $[ATP]_{tot}$ by the following eqation:

$$[ATP] + \frac{K_1[E]_{tot}[ATP]}{1 + K_1[ATP] + K_{MA}K_{Mg}[Mg^{2+}]_{tot}[ATP]} + \frac{K_{Mg}[Mg^{2+}]_{tot}[ATP] + \frac{K_{MA}K_{Mg}[E]_{tot}[Mg^{2+}]_{tot}[ATP]}{1 + K_1[ATP] + K_{MA}K_{Mg}[Mg^{2+}]_{tot}[ATP]} - [ATP]_{tot} = 0 \qquad (A3)$$

Solving for the roots of eq A3 allows [ATP] to be calculated. The concentrations of E1ATP and E1MgATP can then be determined from

$$[E1ATP] = \frac{K_1[E]_{tot}[ATP]}{1 + K_1[ATP] + K_{MA}K_{Mg}[Mg^{2+}]_{tot}[ATP]} \qquad (A4)$$

$$[\mathrm{E1MgATP}] = \frac{K_{MA}K_{Mg}[\mathrm{E}]_{\mathrm{tot}}[\mathrm{Mg}^{2+}][\mathrm{ATP}]}{1 + K_1[\mathrm{ATP}] + K_{MA}K_{Mg}[\mathrm{Mg}^{2+}]_{\mathrm{tot}}[\mathrm{ATP}]} \quad \text{(A5)}$$

The total degree of saturation of the ATP sites under these conditions is given by $S = ([\mathrm{E1ATP}] + [\mathrm{E1MgATP}])/[\mathrm{E}]_{\mathrm{tot}}$.

Cooperative Dimer Model. From stopped-flow kinetic experiments (*16*), it was found that ATP binding was better described by a cooperative binding of two ATP molecules to an enzyme dimer (see Figure 4). Taking into account mass balance for the enzyme, the equilibrium concentrations of enzyme dimer with one and two molecules of ATP bound are given by the following:

$$[\mathrm{E1ATP:E1}] = \frac{K_1[\mathrm{E}]_{\mathrm{tot}}[\mathrm{ATP}]}{1 + 2K_1[\mathrm{ATP}] + K_1K_2[\mathrm{ATP}]^2} \quad \text{(A6)}$$

$$[\mathrm{E1ATP:E1ATP}] = \frac{K_1K_2[\mathrm{E}]_{\mathrm{tot}}[\mathrm{ATP}]^2}{2 + 4K_1[\mathrm{ATP}] + 2K_1K_2[\mathrm{ATP}]^2} \quad \text{(A7)}$$

In eq A6, [E1ATP:E1] represents the sum of the concentrations of the two species E1ATP:E1 and E1:E1ATP. These two species are chemically indistinguishable, but for statistical reasons, it is important to consider both because this takes into account the fact that there are two sites available on a protein dimer for the first ATP molecule to bind whereas there is only one site available for the second ATP molecule. Taking into account mass balance for ATP, [ATP] is related to $[\mathrm{E}]_{\mathrm{tot}}$ and $[\mathrm{ATP}]_{\mathrm{tot}}$ by the following equation:

$$[\mathrm{ATP}] + \frac{K_1[\mathrm{E}]_{\mathrm{tot}}[\mathrm{ATP}] + K_1K_2[\mathrm{E}]_{\mathrm{tot}}[\mathrm{ATP}]^2}{1 + 2K_1[\mathrm{ATP}] + K_1K_2[\mathrm{ATP}]^2} - [\mathrm{ATP}]_{\mathrm{tot}} = 0 \quad \text{(A8)}$$

Solving for the roots of eq A8 allows [ATP] to be calculated and then, by its substitution into eqs A6 and A7, [E1ATP:E1] and [E1ATP:E1ATP] as well.

If one wishes to fit or simulate equilibrium titrations and presteady-state kinetic data, the total degree of saturation, *S*, of the ATP sites for the cooperative dimer model is given by $([\mathrm{E1ATP:E1}] + 2[\mathrm{E1ATP:E1ATP}])/[\mathrm{E}]_{\mathrm{tot}}$. Note that in this expression, as in the case of eq A6, [E1ATP:E1] actually represents the sum of the concentrations of the two species E1ATP:E1 and E1:E1ATP. The fraction of enzyme dimer, S_{dim}, totally saturated with ATP, i.e., in the form E1ATP:E1ATP, is given by $[\mathrm{E1ATP:E1ATP}]/([\mathrm{E}]_{\mathrm{tot}}/2)$.

ACKNOWLEDGMENT

We thank Professor Mikael Esmann, Professor Philippe Champeil, Professor Rolando Rossi, and Professor Steven Karlish for valuable discussions.

REFERENCES

1. Kaplan, J. H. (2002) Biochemistry of Na,K-ATPase. *Annu. Rev. Biochem. 71*, 511–535.
2. Kaplan, J. H. (2004) The Na,K-ATPase: A Current Overview, in *Handbook of ATPases* (Futai, M.; Wada, Y., and Kaplan, J. H., Eds.) pp 89−97, Wiley-VCH Verlag, Weinheim, Germany.
3. Stein, W. D., Lieb, W. R., Karlish, S. J. D., and Eilam, Y. (1973) A model for active transport of sodium and potassium ions as mediated by a tetrameric enzyme. *Proc. Natl. Acad. Sci. U.S.A. 70*, 275–278.
4. Repke, K. R. H., and Schön, R. (1973) Flip-flop model of (NaK)-ATPase function. *Acta Biol. Med. Germ. 31*, K19–K30.
5. Blostein, R. (1975) Na^+ATPase of the mammalian erythrocyte membrane. Reversibility of phosphorylation at 0°. *J. Biol. Chem. 250*, 6118–6124.
6. Ottolenghi, P., and Jensen, J. (1983) The K^+-induced apparent heterogeneity of high-affinity nucleotide-binding sites in (Na^+ + K^+)-ATPase can only be due to the oligomeric structure of the enzyme. *Biochim. Biophys. Acta 727*, 89–100.
7. Esmann, M. (1984) The distribution of $C_{12}E_8$-solubilized oligomers of the (Na^+ + K^+)-ATPase. *Biochim. Biophys. Acta 787*, 81–89.
8. Askari, A. (1987) (Na^+ + K^+)-ATPase: On the number of ATP sites of the functional unit. *J. Bioenerg. Biomembr. 19*, 359–374.
9. Nørby, J. G., and Jensen, J. (1991) Functional Significance of the Oligomeric Structure of the Na,K-Pump from Radiation Inactivation and Ligand Binding, in *The Sodium Pump: Structure, Mechanism, and Regulation* (Kaplan, J. H., and DeWeer, P., Eds.) pp 173−188, Rockefeller University Press, New York, NY.
10. Blanco, G., Koster, J. C., and Mercer, R. W. (1994) The α subunit of the Na,K-ATPase specifically and stably associates into oligomers. *Proc. Natl. Acad. Sci. U.S.A. 91*, 8542–8546.
11. Froehlich, J. P., Taniguchi, K., Fendler, K., Mahaney, J. E., Thomas, D. D., and Albers, R. W. (1997) Complex kinetic behaviour in the Na,K- and Ca-ATPases. *Ann. N.Y. Acad. Sci. 834*, 280–296.
12. Tsuda, T., Kaya, S.,Yokohama, T., Hayashi, Y., and Taniguchi, K. (1998) ATP and acetyl phosphate induces molecular events near the ATP binding site and the membrane domain of Na^+,K^+-ATPase. The tetrameric nature of the enzyme. *J. Biol. Chem. 273*, 24339–24345.
13. Thoenges, D., Amler, E., Eckert, T., and Schoner, W. (1999) Tight binding of bulky fluorescent derivatives of adenosine to the low affinity E_2ATP site leads to inhibition of Na^+/K^+-ATPase. Analysis of structural requirements of fluorescent ATP derivatives with a Koshland-Némethy-Filmer model of two interacting sites. *J. Biol. Chem. 274*, 1971–1978.
14. Taniguchi, K., Kaya, S., Abe, K., and Mårdh, S. (2001) The oligomeric nature of Na/K-transport ATPase. *J. Biochem. 129*, 335–342.
15. Clarke, R. J., Apell, H.-J., and Kong, B. Y. (2007) Allosteric effect of ATP on Na^+,K^+-ATPase conformational kinetics. *Biochemistry 46*, 7034–7044.
16. Clarke, R. J., and Kane, D. J. (2007) Two gears of pumping by the sodium pump. *Biophys. J. 93*, 4187–4196.
17. Brotherus, J. R., Jacobsen, L., and Jørgensen, P. L. (1983) Soluble and enzymatically stable (Na^+ + K^+)-ATPase from mammalian kidney consisting predominantly of protomer αβ-units. Preparation, assay and reconstitution of active Na^+,K^+ transport. *Biochim. Biophys. Acta 731*, 290–303.
18. Jørgensen, P. L., and Andersen, J. P. (1986) Thermoinactivaton and aggregation of αβ units in soluble and membrane-bound (Na,K)-ATPase. *Biochemistry 25*, 2889–2897.
19. Ward, D. G., and Cavieres, J. D. (1996) Binding of 2′(3′)-*O*-(2,4,6-trinitrophenyl)ADP to soluble αβ protomers of Na,K-ATPase modified with fluorescein isothiocyanate. Evidence for two distinct nucleotide sites. *J. Biol. Chem. 271*, 12317–12321.
20. Martin, D. W., and Sachs, J. R. (1999) Preparation of Na^+,K^+-ATPase with near maximal specific activity and phosphorylation capacity: Evidence that the reaction mechanism involves all of the sites. *Biochemistry 38*, 7485–7497.
21. Martin, D. W., Marecek, J., Scarlata, S., and Sachs, J. R. (2000) αβ protomers of Na^+,K^+-ATPase from microsomes of duck salt gland are mostly monomeric: Formation of higher oligomers does not modify molecular activity. *Proc. Natl. Acad. Sci. U.S.A. 97*, 3195–3200.
22. Martin, D. W., and Sachs, J. R. (2000) Ligands presumed to label high affinity and low affinity ATP binding sites do not interact in an $(\alpha\beta)_2$ diprotomer in duck nasal gland Na^+,K^+-ATPase, nor do the sites coexist in native enzyme. *J. Biol. Chem. 275*, 24512–24517.
23. Nørby, J. G., and Jensen, J. (1971) Binding of ATP to brain microsomal ATPase. Determination of the ATP binding capacity and the dissociation constant of the enzyme-ATP complex as a function of K^+ concentration. *Biochim. Biophys. Acta 233*, 104–116.

24. Hegyvary, C., and Post, R. L. (1971) Binding of adenosine triphosphate to sodium and potassium ion-stimulated adenosine triphosphatase. *J. Biol. Chem. 246*, 5234–5240.
25. Fedosova, N. U., Champeil, P., and Esmann, M. (2003) Rapid filtration analysis of nucleotide binding to Na,K-ATPase. *Biochemistry 42*, 3536–3543.
26. Grell, E., Lewitzki, E., Schacht, A., and Stolz, M. (2004) Nucleotide/protein interaction. Energetic and structural features of Na,K-ATPase. *J. Therm. Anal. Cal. 77*, 471–481.
27. Esmann, M., Fedosova, N. U., and Marsh, D. (2008) Osmotic stress and viscous retardation of the Na,K-ATPase ion pump. *Biophys. J. 94*, 2767–2776.
28. Froehlich, J. P., Hobbs, A. S., and Albers, R. W. (1983) Evidence for parallel pathways of phosphoenzyme formation in the mechanism of ATP hydrolysis by electrophorus Na,K-ATPase. *Curr. Top. Membr. Transport 19*, 513–535.
29. Borlinghaus, R., and Apell, H.-J. (1988) Current transients generated by the Na^+/K^+-ATPase after an ATP concentration jump: dependence on sodium and ATP concentration. *Biochim. Biophys. Acta 939*, 197–206.
30. Fendler, K., Jaruschewski, S., Hobbs, A., Albers, W., and Froehlich, J. P. (1993) Pre-steady state charge translocation in NaK-ATPase from eel electric organ. *J. Gen. Physiol. 102*, 631–666.
31. Friedrich, T., Bamberg, E., and Nagel, G. (1996) Na^+,K^+-ATPase pump currents in giant excised patches activated by an ATP concentration jump. *Biophys. J. 71*, 2486–2500.
32. Kane, D. J., Fendler, K., Grell, E., Bamberg, E., Taniguchi, K., Froehlich, J. P., and Clarke, R. J. (1997) Stopped-flow kinetic investigations of conformational changes of pig kidney Na^+,K^+-ATPase. *Biochemistry 36*, 13406–13420.
33. Clarke, R. J., Kane, D. J., Apell, H.-J., Roudna, M., and Bamberg, E. (1998) Kinetics of the Na^+-dependent conformational changes of rabbit kidney Na^+,K^+-ATPase. *Biophys. J. 75*, 1340–1353.
34. Grell, E., Schick, E., and Lewitzki, E. (2001) Membrane receptor calorimetry: cardiac glycoside interaction with Na,K-ATPase. *Thermochim. Acta 380*, 245–254.
35. Skou, J. C., and Esmann, M. (1988) Preparation of membrane Na^+,K^+-ATPase from rectal glands of *Squalus acanthias*. *Methods Enzymol. 156*, 43–46.
36. Ottolenghi, P. (1975) The reversible delipidation of a solubilized sodium-plus-potassium ion-dependent adenosine triphosphatase. *Biochem. J. 151*, 61–66.
37. Peterson, G. L. (1977) A simplification of the protein assay method of Lowry et al. which is more generally applicable. *Anal. Biochem. 83*, 346–356.
38. Lowry, O. H., Rosebrough, N. J., Farr, A. L., and Randall, R. J. (1951) Protein measurement with the Folin phenol reagent. *J. Biol. Chem. 193*, 265–275.
39. Jørgensen, P. L., and Andersen, J. P. (1988) Structural basis for E_1-E_2 conformational transitions in Na,K-pump and Ca-pump proteins. *J. Membr. Biol. 103*, 95–120.
40. O'Sullivan, W. J., and Smithers, G. W. (1979) Stability constants for biologically important metal-ligand complexes. *Methods Enzymol. 63*, 294–336.
41. Fedosova, N. U., Champeil, P., and Esmann, M. (2002) Nucleotide binding to Na,K-ATPase: The role of electrostatic interactions. *Biochemistry 41*, 1267–1273.
42. Montes, M. R., González-Lebrero, R. M., Garrahan, P. J., and Rossi, R. C. (2004) Quantitative analysis of the interaction between the fluorescent probe eosin and the Na^+/K^+-ATPase studied through Rb^+ occlusion. *Biochemistry 43*, 2062–2069.
43. Stürmer, W., and Apell, H.-J. (1992) Fluorescence study on cardiac glycoside binding to the Na,K-pump. *FEBS Lett. 300*, 1–4.
44. Kane, D. J., Grell, E., Bamberg, E., and Clarke, R. J. (1998) Dephosphorylation kinetics of pig kidney Na^+,K^+-ATPase. *Biochemistry 37*, 4581–4591.
45. Klodos, I., and Skou, J. C. (1977) The effect of chelators on Mg^{2+}, Na^+-dependent phosphorylation of ($Na^+ + K^+$)-activated ATPase. *Biochim. Biophys. Acta 481*, 667–679.
46. Dawson, R. M. C.; Elliott, D. C.; Elliott, W. H., and Jones, K. M. (1986) *Data for Biochemical Research*, 3rd ed., pp 399−415, Oxford University Press, Oxford, UK.
47. Campos, M., and Beaugé, L. (1992) Effects of magnesium and ATP on pre-steady-state phosphorylation kinetics of the Na^+,K^+-ATPase. *Biochim. Biophys. Acta 1105*, 51–60.
48. Keillor, J. W., and Jencks, W. P. (1996) Phosphorylation of the sodium-potassium adenosinetriphosphatase proceeds through a rate-limiting conformational change followed by rapid phosphoryl transfer. *Biochemistry 35*, 2750–2753.
49. Ghosh, M. C., and Jencks, W. P. (1996) Phosphorylation of the sodium-potassium adenosinetriphosphatase with adenosine triphosphate and sodium ion that requires subconformations in addition to principal E_1 and E_2 conformations of the enzyme. *Biochemistry 35*, 12587–12590.
50. Lüpfert, C., Grell, E., Pintschovius, V., Apell, H.-J., Cornelius, F., and Clarke, R. J. (2001) Rate limitation of the Na^+,K^+-ATPase pump cycle. *Biophys. J. 81*, 2069–2081.
51. Cornelius, F. (1999) Rate determination in phosphorylation of shark rectal Na,K-ATPase by ATP: Temperature sensitivity and effects of ADP. *Biophys. J. 77*, 934–942.
52. Bernasconi, C. F. (1976) *Relaxation Kinetics*, pp 3−12, Academic Press, New York.
53. Olesen, C., Picard, M., Winther, A.-M. L., Gyrup, C., Morth, J. P., Oxvig, C., Møller, J. V., and Nissen, P. (2007) The structural basis of calcium transport by the calcium pump. *Nature 450*, 1036–1044.
54. Morth, J. P., Pedersen, B. P., Toustrup-Jensen, M. S., Sørensen, T. L.-M., Petersen, J., Andersen, J. P., Vilsen, B., and Nissen, P. (2007) Crystal structure of the sodium-potassium pump. *Nature 450*, 1043–1050.
55. Møller, J. P., Lind, K. E., and Andersen, J. P. (1980) Enzyme kinetics and substrate stabilization of detergent-solubilized and membranous ($Ca^{2+} + Mg^{2+}$)-activated ATPase from sarcoplasmic reticulum. Effect of protein-protein interactions. *J. Biol. Chem. 255*, 1912–1920.
56. Mimura, K., Tahara, Y., Shinji, N., Tokuda, E., Takenaka, H., and Hayashi, Y. (2008) Isolation of stable $(\alpha\beta)_4$-tetraprotomer from Na^+/K^+-ATPase solubilized in the presence of short-chain fatty acids. *Biochemistry 47*, 6039–6051.
57. Yokoyama, T., Kaya, S., Abe, K., Taniguchi, K., Katoh, T., Yazawa, M., Hayashi, Y., and Mårdh, S. (1999) Acid-labile ATP and/or ADP/P_i binding to the tetraprotomeric form of Na/K-ATPase accompanying catalytic phosphorylation-dephosphorylation cycle. *J. Biol. Chem. 274*, 31792–31796.

BI801593G